Does Green Light Influence the Fluorescence Properties and Structure of Phototrophic Biofilms?

1. **M. Roldán**[1],
2. **F. Oliva**[2],
3. **M. A. Gónzalez del Valle**[3],
4. **C. Saiz-Jimenez**[3] **and**
5. **M. Hernández-Mariné**[1,*]

1. [1]Departament de Productes Naturals, Biologia Vegetal i Edafologia, Universitat de Barcelona, Av. Joan XXIII s/n, 08028 Barcelona, Spain
2. [2]Departament d'Estadística, Facultat de Biologia, Universitat de Barcelona, Av. Diagonal 645, 08028 Barcelona, Spain
3. [3]Instituto de Recursos Naturales y Agrobiologia, CSIC, Sevilla, Spain

ABSTRACT

Artificial illumination can harm works of art by inducing the development of photosynthetic biofilms. With the aim of preventing biodeterioration or esthetic damage to such surfaces, we evaluated and compared the effects of illuminating biofilms formed by *Gloeothece membranacea* (cyanobacteria) and *Chlorella sorokiniana* (Chlorophyta) using exclusively white or green light.

Inappropriate artificial illumination of archaeological remains and their interior works of art (1, 2, 3, 4) results in the uncontrolled development of photosynthetic microorganisms, primarily cyanobacteria and microalgae (10, 13, 15, 19, 20), forming greenish biofilms that contribute to surface biodeterioration. These organisms feature a matrix composed primarily of exopolymers (EPS) that are involved in the resistance of biofilms to adverse abiotic conditions as well as in attachment (3, 5, 6, 24). Owing to their hygroscopicity (7, 8, 11, 28), EPS can be particularly harmful to archaeologically valuable surfaces. Control efforts usually focus on cleaning damaged surfaces or on chemical treatments that have little efficacy against biofilms (5, 14). Hence, there is an ever-increasing interest in the development of alternative strategies for preventing and minimizing biofilm development.

Changes in spectral ambient light produce variations in pigment distribution and abundance for cyanobacteria and microalgae (17, 18, 23). In particular, green light (GL) retards growth (9), causes vacuolation in the thylakoidal system (1), and affects pigment composition (25) and fine structure (1). GL is also advantageous since it represents the maximum absorbance of human vision. We thus sought to evaluate the potential for GL to prevent biofilm growth by comparing the responses of artificial biofilms exposed to either GL or white light (WL).

Biofilm preparation.

Sterilized lime-pozzolana slabs (three slabs, 3 by 1 cm) were inoculated with 1 g of a mixture of *Gloeothece membranacea* Bornet CCAP1430/3 (Pasteur Culture Collection, Paris, France) and *Chlorella sorokiniana* Shih and Krauss SAG 211-32 (Centro de Investigaciones Cientificas, Isla de La Cartuja, Seville,

Spain). The slabs were placed in petri dishes and stored at 19 to 22°C under continuous GL (Narva LT 18 W/017 green TT; Narva, Czech Republic) or WL (Chiyoda F 15 S daylight; Chiyoda Corporation, Japan) at a constant photon flux density of 20 μmol · m^{-2} · s^{-1} for 60 days. The emission spectra of the lamps were measured with a LICOR (Lincoln, NE) Li-1800 spectroradiometer (Fig. 1).

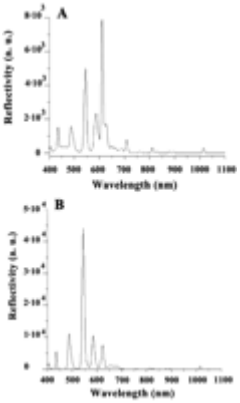

View larger version:
FIG. 1.

Spectral emission of the two fluorescent light sources, white (A) and green (B) light, in the 400- to 1,100-nm range at a photon flux density of 20 μmol · m^{-2} · s^{-1}. In addition to a peak at 544 nm, the green lamps gave two small shoulders at 425 to 450 nm and at 480 to 510 nm, wavelengths at which PC and PE absorb energy.

CSLM.

Confocal scanning laser microscopy (CSLM) was performed to establish possible differences between GL and WL treatments in morphology, size of thylakoidal areas, and architecture of biofilms (20), for which a Leica TCS-SP2 (Leica Microsystems Heidelberg GmbH, Mannheim, Germany) was used. Autofluorescence from photosynthetic pigments (PP) was excited with the 543- and 633-nm lines of an Ar/HeNe laser and observed in the red channel at an emission range of 590 to 800 nm. EPS were labeled with the carbohydrate-recognizing lectin concanavalin A (ConA)-Alexa Fluor 488 (Molecular Probes, Inc., Eugene, OR), excited with the 488-nm line of an Ar laser, and viewed in the green channel at 490 to 530 nm. Unlabeled organisms were used for a staining control. To determine the spatial relationship between pigment fluorescence and EPS, bichannel images were acquired in the *x-y* plane at different intervals along the *z* axis. The thickness of the sample was established as the distance from the highest position to the lowest position of inherent pigment fluorescence. Image combining and processing were performed with the Imaris software package, version 2.7 (Bitplane AG, Zürich, Switzerland) (20).

Analysis of organisms.

Slabs maintained under GL exhibited colonies of two to four cells of *G. membranacea* surrounded by a relatively thick sheath in which only the oldest wrecked external layers were labeled by ConA (Fig. 2A). Membrane vacuolized thylakoids were seen as empty spaces inside the cells (Fig. 2C). Slabs kept under WL displayed *G. membranacea* colonies with a larger number of cells (with 54.1% having more than four cells) surrounded by an apparently compact sheath that was strongly labeled in green in all layers (Fig. 2B); *C. sorokiniana* was nearly absent in slabs maintained under GL (Fig. 2A and C), showing negative selection under this spectral quality (27).

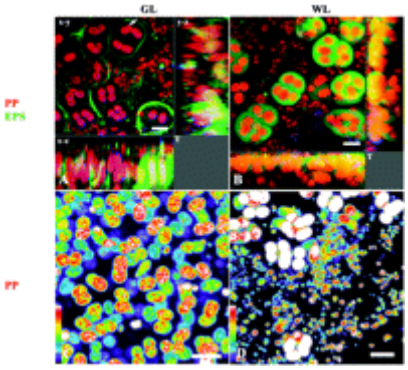

View larger version:

FIG. 2.

CSLM three-dimensional images of biofilms under GL and WL conditions. The color assignment in the figures is red for PP and green for ConA lectin conjugated with Alexa Fluor 488-labeled EPS. (A) Detail of *Gloeothece membranacea* colonies grown in GL. Shown is a bichannel extended-focus projection of 232 *x-y* optical sections (*z* step = 0.2 μm). (B) Details of *G. membranacea* colonies grown in WL. *Chlorella sorokiniana* was found in the upper layer (T). Shown is a bichannel extended-focus projection of 142 *x-y* optical sections (*z* step = 0.2 μm). (C and D) False color representation corresponding to the pigment autofluorescence. The color key is shown at the bottom left. (C) Thylakoidal PP in *G. membranacea*. Shown is a bichannel maximum intensity projection of 73 *x-y* optical sections (*z* step = 0.2 μm). (D) Cells of *G. membranacea* and *C. sorokiniana*. Shown is a maximum intensity projection of 139 *x-y* optical sections (*z* step = 0.2 μm). T, biofilm surface. Scale bar, 10 μm.

Metamorph software (Universal Imaging Corp.) was used to measure pigment fluorescence regions in three-dimensional projections of unlabeled cells. Data sets were exported into Microsoft Excel for analysis. In GL, the mean dimensions (length by width) for *G. membranacea* (26 cells) were 6.23 ± 1.32 μm by 4.52 ± 0.40 μm; in WL (17 cells), the mean dimensions were 6.91 ± 1.77 μm by 5.42 ± 0.55 μm. For *C. sorokiniana*, the mean dimensions under GL (48 cells) were 3.18 ± 0.52 μm by 2.65 ± 0.57 μm; in WL, the mean dimensions (54 cells) were 3.43 ± 0.71 μm by 2.88 ± 0.6 μm. The results for each species were processed with a one-way analysis of variance (ANOVA) model using SAS software. Thylakoid region width for *G. membranacea* in GL compared to that in WL ($F_{1, 41}$ = 38.12; P = 0.000) and the thylakoid region length ($F_{1, 100}$ = 4.09; P = 0.046) and width ($F_{1, 100}$ = 3.83; P = 0.053) for *C. sorokiniana* were statistically

significantly smaller. Both species exhibited restricted cell volume, a strategy used by organisms to decrease energy demands (26).

Analysis of biofilms.

Quantitative analysis of biofilm structure was carried out with the GNU Public License program (Departament de Llenguatges i Sistemes Informàtics, Universitat Politècnica de Catalunya [https://lafarga.cpl.upc.edu/projects/qbiof/]) based on the Comstat software package (12). Both GL- and WL-grown biofilms (Fig. 2 and Table 1) were formed by a layer of *G. membranacea*, with the colonies being thinner and more compact in WL (Fig. 2A and B). For biofilms exposed to GL, *C. sorokiniana* was scarce (Fig. 2A and C), whereas in WL (Fig. 2B and D), it had an irregular density. PP biovolume ($\mu m^3 \cdot \mu m^{-2}$) was larger for GL biofilms (Table 1), whereas the PP roughness coefficient, which provides a measure of how much the thickness of the biofilm varies, and PP biofilm porosity (16) were much lower than in WL (Table 1). The EPS porosity and roughness coefficient were higher in GL than in WL (Table 1).

TABLE 1.

Quantitative analysis of biofilm structure[a]

ConA labeling of *G. membranacea* grown in WL suggests that its EPS contain α-d-mannose and/or α-d-glucose residues, sugars to which ConA binds with high specificity (22). In GL, EPS of this type were not produced; the labeled outer rings correspond to remains from the original culture. The low efficiency of light absorption of chlorophyll (Chl) *a* in GL for *G. membranacea* biofilms and the concomitant changes in EPS production (8, 22) would result in a weaker attachment to the substratum (6, 11) and a reduction in tolerance to desiccation stress (24).

Analysis of pigment fluorescence: lambda scan function.

The fluorescence spectra of pigments were obtained in single cells from the intact biofilms by a noninvasive method (21) using a Leica TCS-SP2 microscope. Gains and offsets were equal for each field at different excitation wavelengths (λ_{exc}s) and remained constant during the scanning process. To determine the spectral signature of a selected area from the scanned image (Fig. 3A and 4A), 1-μm^2 regions of interest (ROIs) taken from the thylakoid region inside the cell were established for each *x*-*y*-λ stack of images.

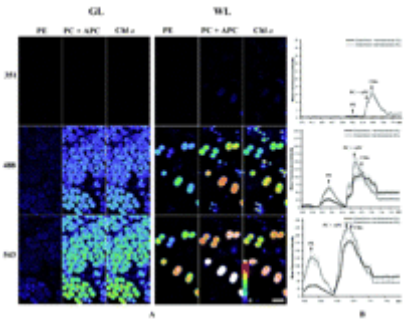

FIG. 3.

In vivo CSLM images and lambda scans of *Gloeothece membranacea*. Optical sections and spectral profiles derived from λ_{exc}s of 351, 488, and 543 nm under WL and GL conditions. (A) False color representation corresponding to the λ_{max} autofluorescence of Chl *a* and phycobiliproteins from WL and GL spectral data sets for each of the three λ_{exc}s. The color key is shown at the bottom right. Such optical sections correspond to the maximum peak when excited with the corresponding λ_{exc}, shown in the plots in B (arrows). (B) Two-dimensional plots representing the MFI spectra for *G. membranacea* under WL and GL conditions. Data are the means ± standard errors from 20 cells of the three fields examined in each treatment. PC + APC, phycocyanin plus allophycocyanin. Scale bar, 10 μm.

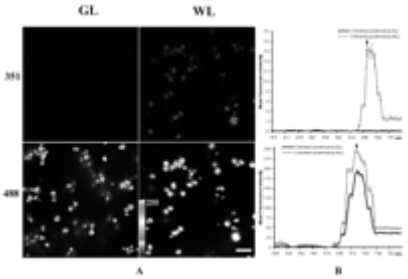

FIG. 4.

In vivo CSLM images and lambda scans of *Chlorella sorokiniana*. Optical sections and spectral profiles derived from λ_{exc}s of 351 and 488 nm under WL and GL conditions are shown. (A) False color representation corresponding to the λ_{max} autofluorescence of Chl *a* and *b* from WL and GL spectral data sets for each of the two λ_{exc}s. The color key is shown at the bottom right. Optical sections correspond to the maximum peak when excited with the corresponding λ_{exc}s, shown in the plots in B (arrows). (B) Two-dimensional plots representing the MFI spectra for *C. sorokiniana* under WL and GL conditions. Data are the means ± standard errors from 20 cells of the three fields examined in each treatment. Note the decrease in MFI of the pigments from GL treatment relative to the WL control. Scale bar, 10 μm.

Lambda scans of both species (*n* = 20 ROIs) obtained for each λ_{exc} in at least three independent experiments show that mean fluorescence intensity (MFI) and the half-bandwidth of the spectra from both species were different for both light types, whereas the spectrum shapes were identical (Fig. 3 and 4).

In GL, the fluorescence spectra for all pigments in both species at all λ_{exc}s were less intense than those for WL (Fig. 3A and 4A). Both species grown under WL emitted only red fluorescence of Chl *a* when excited with UV light (351 nm) (Fig. 3A and 4A).

***Gloeothece membranacea*.**

In both WL and GL, fluorescence was weaker at a λ_{exc} of 488 nm (blue region) than at a λ_{exc} of 543 nm, where the Chl *a* receives its energy from phycobilins (20). C-phycoerythrin (PE) showed fluorescence at an emission wavelength of ca. 580 nm when excited at 488 nm and at its optimum λ_{exc} (543 nm). Upon

comparison of the MFI at λ_{exc}s of 488 and 543 nm in both treatments, the MFI was observed to be lower in the blue region (Fig. 3B).

For the GL sample, the highest maximum for *G. membranacea* corresponded to Chl *a* (ca. 670.7 nm), and its strongest emission was at a λ_{exc} of 488 nm. The content of PE pigment was higher than in WL, which has previously been reported as a response to low light or as a chromatic adaptation, allowing the organism to harvest light from the green-yellow bandwidths (18, 28).

The emission bands for WL samples were considerably higher (659.3 to 666.4 nm) than those for GL samples, corresponding to the phycobiliproteins C-phycocyanin (PC) and allophycocyanin (APC) (Fig. 3B); however, the proportion of Chl *a* fluorescence to total pigment fluorescence was much lower.

***Chlorella sorokiniana*.**

At a λ_{exc} of 488 nm, differences in the Chl *a* maximum (λ_{max} = 687.9 nm) were not observed for samples of either light type (Fig. 4).

The mean and standard error were calculated for all the ROIs examined at each λ_{exc}. For each species and line, the significance of the results was evaluated with a repeated measures ANOVA model. Three factors were taken into account: light treatment, emission wavelength, and cell. The cell factor is nested into the light treatment, and emission wavelength is the repeated measures factor ("within-subject effects" due to the fact that every cell is measured at all wavelengths). All three factors had statistically significant differences ($P < 0.05$ in all cases) for the two species at every line (351, 488, and 543 nm).

At a λ_{exc} of 351 nm, significant differences in MFI were found for the emission range of 649.5 to 683.4 nm, in which PC, APC, and Chl *a* emit. At a λ_{exc} of 488 nm, significant differences in MFI were found for the emission range of 573.6 to 590.7 nm, in which PE emits, and 653.6 to 659.3 nm, in which PC and APC emit. Finally, at a λ_{exc} of 543 nm, significant differences in MFI were found for the emission range of 567.8 to 598.8 nm, in which PE emits, 645.3 to 668.6 nm, in which PC and APC emit, and 684.1 nm, in which Chl *a* emits. Statistical analysis confirmed the significance of the results outlined above (Table 2).

TABLE 2.

Three-way ANOVA of *G. membranacea* and *C. sorokiniana* in the different λ_{exc}s[a]

Conclusions.

The observations reported above suggest that GL could prevent the growth of photosynthetic organisms, except for those capable of modifying accessory pigments. However, even biofilms composed of the chromatic adaptable phycoerythrin-containing *G. membranacea* had lower photosynthetic pigment biovolume, smaller thylakoid regions, and a weaker MFI in GL than in WL, all of which are signs of retarded growth and thus suggest a possible treatment for

preventing photosynthetic biofilm growth. Although laboratory data cannot be extrapolated to natural environments, our results have prompted studies of the application of green light to artificially illuminated works of art.

ACKNOWLEDGMENTS

This work was supported by the EU Programme for Energy, Environment, and Sustainable Development in the CATS Project, contract EVK4-CT-2000-00028.

We thank the Scientific and Technical Services of the University of Barcelona for their excellent technical assistance with the CSLM and the Department of Fluid Mechanics Energy Engineering at the Superior School of Engineering of the University of Seville for their assistance with the spectral measurements of light sources.

REFERENCES

Albertano, P. *1991. Effects of monochromatic lights on four species of Leptolyngbya. Arch. Hydrobiol. Algol. Stud. 64:199-214.*

Albertano, P., and L. Bruno. *2003. The importance of light in the conservation of hypogean monuments, p. 171-177. In C. Saiz-Jiménez (ed.), Molecular biology and cultural heritage. Swets & Zeitlinger, Lisse, The Netherlands.*

Albertano, P., D. Moscone, G. Palleschi, B. Hermosin, C. Saiz-Jiménez, S. Sánchez-Moral, M. Hernández-Mariné, C. Urzí, I. Groth, V. Schroeckh, J. R. Gallon, F. Graziottin, F. Bisconti, and R. Giuliani. *2003. Cyanobacteria attack rocks (CATS): control and preventive strategies to avoid damage caused by cyanobacteria and associated microorganisms in Roman hypogean monuments, p. 151-162. In C. Saiz-Jiménez (ed.), Molecular biology and cultural heritage. Swets & Zeitlinger, Lisse, The Netherlands.*

Ariño, X., M. Hernández-Mariné, and C. Saiz-Jiménez. *1997. Colonization of Roman tombs by calcifying cyanobacteria. Phycologia 36:366-373.*

Costerton, J. W., P. S. Stewart, and E. P. Greenberg. *1999. Bacterial biofilms: a common cause of persistent infections. Science 284:1318-1322.*

Decho, A. W. *2000. Microbial biofilms in intertidal systems: an overview. Cont. Shelf Res. 20:1257-1273.*

De los Ríos, A., C. Ascaso, J. Wierzchos, E. Fernández-Valiente, and A. Quesada. *2004. Microstructural characterization of cyanobacterial*

mats from the McMurdo Ice Shelf, Antarctica. Appl. Environ. Microbiol. 70:569-580.

De Philippis, R., and M. Vicenzini. *1998. Exocellular polysaccharides from cyanobacteria and their possible applications. FEMS Microbiol. Rev. 22:151-175.*

Hauschild, C. A., H. J. McMurter, and F. R. Pick. *1991. Effect of spectral quality on growth and pigmentation of picocyanobacteria. J. Phycol. 27:698-702.*

Hernández-Mariné, M., E. Clavero, and M. Roldán. *2003. Why there is such luxurious growth in the hypogean environments. Arch. Hydrobiol. Algol. Stud. 109:229-239.*

Hernández-Mariné, M., and M. Roldán. *2005. Adherence of hormogonia to substrata is mediated by polysaccharides produced by necridic cells. Arch. Hydrobiol. Algol. Stud. 117:239-249.*

Heydorn, A., A. T. Nielsen, M. Hentzer, C. Sternberg, M. Givskov, B. K. Ersboll, and S. Molin. *2000. Quantification of biofilm structures by the novel computer program COMSTAT. Microbiology 146:2395-2407.*

Hoffmann, L. *2002. Caves and other low-light environments: aerophytic photoautotrophic microorganisms, p. 835-843. In G. Bitton (ed.), Encyclopedia of environmental microbiology. John Wiley & Sons, New York, N.Y.*

Kumar, R., and A. Kumar. *1999. Biodeterioration of stone in tropical environments. An overview. The Getty Conservation Institute, Los Angeles, Calif.*

Lefevre, M. *1974. La maladie verte de Lascaux. Stud. Conserv. 19:126-156.*

Lewandowski, Z. *2000. Notes on biofilm porosity. Water Res. 34:2620-2624.*

Millie, D. F., D. A. Ingram, and C. P. Dionigi. *1990. Pigment and photosynthetic responses of Oscillatoria agardhii (Cyanophyta) to photon flux density and spectral quality. J. Phycol. 26:660-666.*

Mullineaux, C. W. *2001. How do cyanobacteria sense and respond to light? Mol. Microbiol. 41:965-971.*

Ortega-Calvo, J. J., M. Hernández-Mariné, and C. Saiz-Jiménez. *1993. Cyanobacteria and algae on historic buildings and monuments, p. 173-203. In K. L. Garg, H. Arai, and B. Rai (ed.), Recent advances in biodeterioration and biodegradation, vol. I. Naya Prokash, Calcutta, India.*

Roldán, M., E. Clavero, S. Castel, and M. Hernández-Mariné. *2004. Biofilms fluorescence and image analysis in hypogean monuments research. Arch. Hydrobiol. Algol. Stud. 111:127-143.*

Roldán, M., F. Thomas, S. Castel, A. Quesada, and M. Hernández-Mariné. *2004. Noninvasive pigment identification in living phototrophic biofilms by confocal imaging spectrophotometry. Appl. Environ. Microbiol. 70:3745-3750.*

Schüßler, A., T. Meyer, H. Gehrig, and M. Kluge. *1997. Variations of lectin binding sites in extracellular glycoconjugates during the life cycle of Nostoc punctiforme, a potentially endosymbiotic cyanobacterium. Eur. J. Phycol. 32:233-239.*

Talarico, L. *1996. Phycobiliproteins and phycobilisomes in red algae: adaptive responses to light. Sci. Mar. 60:205-222.*

Tamaru, Y., Y. Takani, T. Yoshida, and T. Sakamoto. *2005. Crucial role of extracellular polysaccharides in desiccation and freezing tolerance in the terrestrial cyanobacterium Nostoc commune. Appl. Environ. Microbiol. 71:7327-7333.*

Tandeau de Marsac, N., D. Mazel, T. Damerval, G. Guglielmi, V. Capuano, and J. Houmard. *1988. Photoregulation of gene expression in the filamentous cyanobacterium Calothrix sp. PCC7601. Photosynth. Res. 18:99-132.*

Thompson, P. A., P. J. Harrison, and J. S. Parslow. *1991. Influence of irradiance on cell volume and carbon quota for ten species of marine phytoplankton. J. Phycol. 27:351-360.*

Vila, X., and C. A. Abella. *2001. Light-harvesting adaptations of planktonic phototrophic microorganisms to different light quality conditions. Hydrobiologia 452:15-30.*

Wotton, R. S. *2004. The ubiquity and many roles of exopolymers (EPS) in aquatic systems. Sci. Mar. 68:13-21.*

doi: 10.1128/AEM.72.4.3026-3031.2006 *Appl. Environ. Microbiol. April 2006 vol. 72 no. 4 3026-3031*